

# An Optimized Frequency Locking Loop Employing FM Spectroscopy for a CPT Based Atomic Clock

Ido Ben-Aroya, Matan Kahanov and Gadi Eisenstein

Electrical Engineering department  
Technion-Israel Institute of Technology  
Haifa, Israel  
bido@tx.technion.ac.il

**Abstract**— We present an experimental optimization of the frequency modulation spectroscopy parameters used for a locking loop of a CPT based atomic clock. The optimized operating conditions yield a feedback signal with the largest obtainable signal to noise ratio with which we achieve state of the art clock performance in a system employing a miniature glass Rubidium vapor cell.

## I. INTRODUCTION

Miniature atomic clocks with volumes approaching few cubic centimeters and with a power consumption of only few tens of milli watts have been researched extensively in the past few years [1]. Most these small scale clocks employ a narrow atomic resonance induced by Coherent Population Trapping (CPT) in either Cesium or Rubidium vapor. The CPT process is induced by a vertical cavity surface emitting laser (VCSEL) [2, 3] which is directly modulated at half the hyperfine splitting frequency of the atoms. The first order side bands of the modulated VCSEL serve as the two coherent optical fields needed to excite the dark resonance [4]. The small size of the atomic cell, together with various instabilities of the VCSEL [5], require complex locking schemes [6] in order to achieve an acceptable clock performance. The locking processes usually rely on the resonant absorption but the dispersive nature of the CPT process can also be harnessed for the implementation of an atomic clock.

This paper reports on an experimental  $^{87}\text{Rb}$  CPT based clock which uses a small spherical glass cell [7] and employs the dispersive features of the CPT resonance for the clock locking. Superimposing low rate frequency modulation (FM) on the microwave drive signal to the diode laser enables to probe the atomic vapor using the FM spectroscopy scheme [8, 9, 10]. This spectroscopic technique which employs Lock-in detection yields two outputs: the “in-phase” and “quadrature” signals. A linear superposition of the two components which results from a simple rotational transformation yields the FM spectroscopy parameters (FM modulation-frequency and index) that maximize the sensitivity of the feedback signal in the Frequency-Locked Loop (FLL).

Section II of this paper describes an experimental optimization of the FM spectroscopy parameters. A relatively wide range of parameters is found where high sensitivities and low accompanying noise levels are possible. The performance of a CPT based Rubidium clock which employs optimized FM parameters is presented in section III. The clock exhibits a short-term stability of  $3 \times 10^{-11}/\sqrt{\tau}$  for time constants of 0.5 sec to 200 sec. The relative frequency stability is better than  $10^{-10}$  with a slow drift of only  $10^{-11}$  per day.

## II. EXPERIMENTAL OPTIMIZATION OF THE FREQUENCY-LOCKED LOOP

A key parameter determining the performance of a locked system is the Signal to Noise Ratio (SNR) of the feedback (error) signal [11]. The SNR of the error signal in the system we present was found to depend on the FM spectroscopy parameters. Optimized parameters were determined by scanning a wide range of modulation frequencies and indexes and determining for each set the optimum phase difference between the measurement and reference input signals of the Lock-in amplifier. The noise of the Lock-in amplifier was also measured for each point so that operating conditions for the largest SNR could be determined. Optimized operation could be achieved for well defined sets of FM spectroscopy parameters.

The schematic of the complete atomic clock is shown in fig. 1. A 780.24 nm VCSEL is driven by a DC bias and a microwave signal at a half the  $^{87}\text{Rb}$  hyperfine splitting frequency: 3417.3 MHz. The VCSEL output is collimated and its polarization is set to be circular. The light impinges a ball shaped glass cell with a diameter of 6 mm which contains a mixture of pure  $^{87}\text{Rb}$  atoms and a buffer gas. The cell, together with a controlled heater and a solenoid are placed in a three-layer  $\mu$ -metal box which attenuates the environmental magnetic field. The cell temperature is stabilized around the optimum temperature of  $66^\circ\text{C}$  to a level of 1 mK. A homogeneous magnetic field of 35  $\mu\text{T}$  pointing in a direction parallel to the optical axis is generated around the vapor cell by the solenoid. This magnetic field lifts the Zeeman

The clock system uses two control loops: the VCSEL wavelength stabilization servo loop and the FLL or the clock-loop. The first loop, which appears in the bottom of fig. 1, stabilizes the emitted wavelength by changing the diode laser bias. Various noisy features of the CPT process require detuning the locking point relative to the peak [12]. A red shift of approximately 60 MHz is used in the present system. The second (upper) clock-loop is kept open for the FM spectroscopy characterization while the input voltage to the Oven Controlled Voltage Controlled Crystal Oscillator (OCXO) is stabilized around a fixed value. The loop is closed when the clock is operated using an additional PI controller (shown in a dashed line).

The shapes of the “in-phase” and ‘quadrature’ components are strongly dependent on the phase of the reference signal. Therefore, maximization of the slope of each component near its zero crossing point (around the resonance frequency) requires optimization of the reference phase. Changing the phase of the reference signal by a certain angle is equivalent to a rotational transformation of the two outputs by the opposite angle.

A two step optimization procedure was employed. First, the FM spectroscopy parameters were scanned over a wide range. Modulation frequencies between 300 Hz and 1200 Hz were used while the modulation indexes varied from 0.1 to 2.0. For each of the 85 points we examined the two Lock-in amplifier outputs while the phase reference was held constant. The slope near the zero crossing for each output was then easily determined. Keeping the reference phase unchanged yields a clear optimum modulation frequency and index where the slope at resonance reaches its maximum value.

In the second stage of the procedure, we rotated the two components (obtained for each FM spectroscopy parameter set) with respect to each other in order to obtain the maximum slope around the resonance frequency of the “in-phase” component. The result is presented in fig. 3 as a 3D plot and also in contour form. The figure describes the maximum obtainable slope as a function of the FM parameters where each point was obtained with its corresponding optimized reference phase. The optimized rotation angles are described in a contour form in fig. 4.

Fig. 3 reveals that the maximum slope is achieved along a continuous curve in the FM parameters space. The same maximum value can be achieved for each modulation-frequency by choosing a proper modulation-index and a particular reference phase. Higher modulation frequencies require lower modulation indexes with the index converging asymptotically towards a value of about 0.5.

The physical reasoning behind the observed behavior is related to the fact that the CPT resonance results from a combined interaction of several pairs of spectral lines (see fig. 2a). Since the operating conditions of the cell, and therefore the properties of the obtained resonance remain approximately unchanged, different modulation frequencies require different amplitude distributions among the interacting spectral lines and those are reached by varying the modulation index.

Examining the optimum added reference phase (fig. 4) shows two distinct regions. In one, the contour lines are approximately horizontal. Here, for a constant modulation frequency, the phase increases almost linearly with increasing modulation index at a rather small rate. For a given modulation index, the phase decreases with increasing frequency in a nonlinear manner. The second region, which exhibits almost vertical contour lines, represents sharp phase changes occurring under those conditions where the slope near the zero crossing flips sign due to a basic feature of FM spectroscopy.

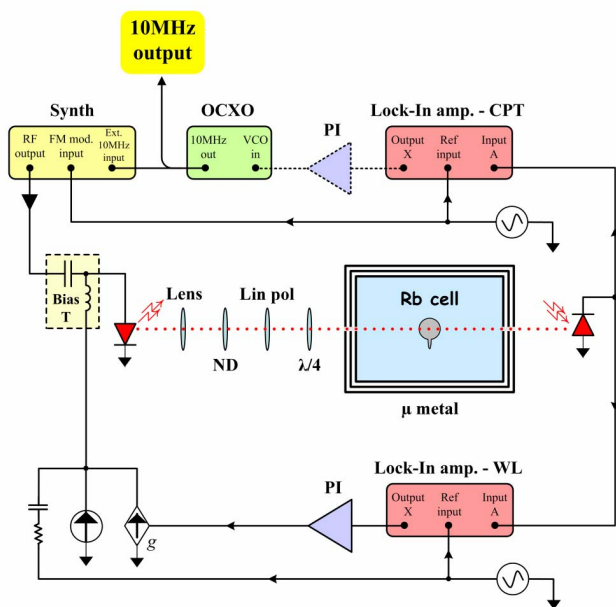


Figure 1. System schematic. The FLL is closed by the dashed line.

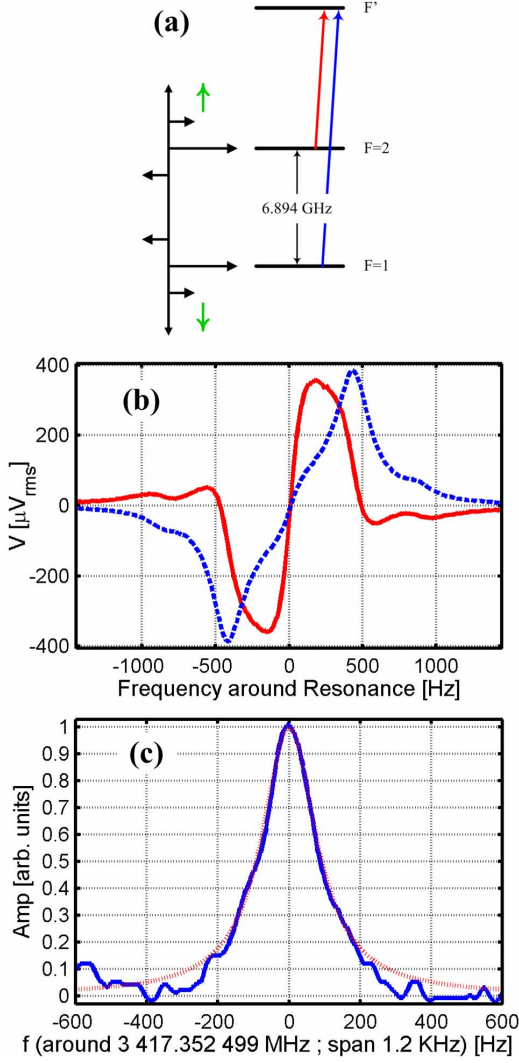


Figure 2. (a) The atomic energy structure and the FM modulated spectrum. (b) Typical Lock-in amplifier output signals while measuring a CPT resonance using the FM spectroscopy technique. The blue dashed line refers to the “in-phase” component while the red line represents the ‘quadrature’. (c) A direct measurement of the CPT resonance (without FM). The measured resonance (the blue line) fits a Lorentzian with a width of 186 Hz (red dotted line).

The variation of the optimum added phase stems from two main effects: the nature of spectroscopy technique and the response of the modulated diode laser. A theoretical analysis of FM spectroscopy where two modulated fields (see fig. 2a) probe a narrow resonance [13] demonstrates the observed dependence of the optimum phase on the FM parameters. In addition, the phase transmission function of the modulated VCSEL is modified by the low-frequency FM modulation of the drive current. Consequently, the phase of the emitted electric field is changed and should be compensated for by the Lock-in amplifier reference phase.

For each FM parameter set, we also measured the accompanying noise by using the noise measurement feature of the Lock-in amplifier. The noise in the ‘quadrature’

component is shown in fig. 5 in contour form. The figure reveals an essentially constant and low noise level in the entire space of FM parameters. The noise of the feedback signal has therefore not effect on the choice of optimum FM parameters.

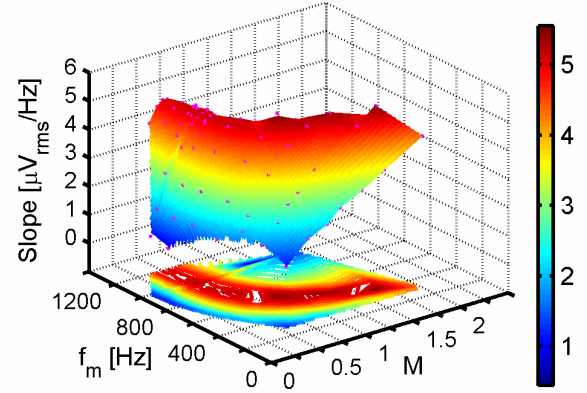


Figure 3. The maximum measured slope which can be achieved by rotating the two Lock-in amplifier output components.

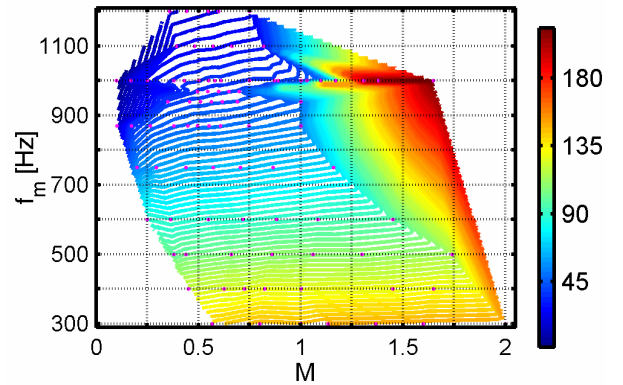


Figure 4. The optimized rotation angle vs. FM parameters.

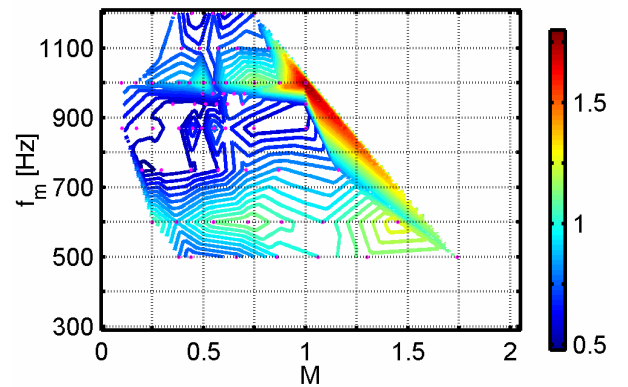


Figure 5. Noise measurements accompanying the ‘quadrature’ components.

### III. CLOCK PERFORMANCE

Using one set of optimized FM parameters (modulation frequency of 870 Hz and an index of 0.5), we constructed the CPT based atomic clock. While a feedback signal with a large SNR can be obtained for many other FM parameters, we chose to operate at a relatively high frequency because it ensures a fast response of the closed loop using a wide bandwidth low pass filter in the Lock-in amplifier.

The clock loop (upper loop in fig. 1) was stabilized on the zero crossing point of the steep FM spectroscopy output signal near the resonance frequency. In the locked state, the error signal fed a 10 MHz OCXO through a PI controller. This OCXO serves as the reference for the microwave source driving the diode laser and it also provides the stabilized 10 MHz output of the clock.

The short-term performance of the clock is described in fig. 6. Shown is the measured Allan deviation with a short-term stability of  $3 \times 10^{-11}/\sqrt{\tau}$  for time constants of 0.5 sec to 200 sec. The Allan deviation reaches a minimum at about 500 sec and then increases gradually.

Long term frequency stability was also tested. The 10 MHz output was sampled every few seconds over more than 24 hours. The results shown in fig. 7 demonstrate that the frequency deviates by less than  $\pm 1$  mHz with a slow drift of approximately 0.1 mHz per day.

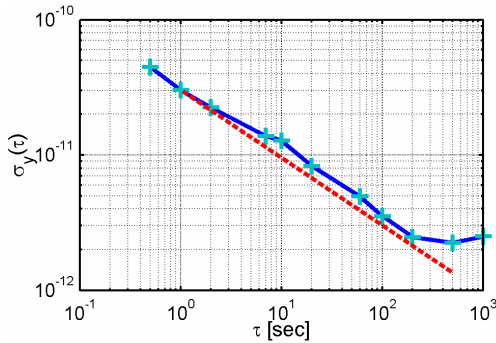


Figure 6. Measured Allen deviation of the CPT based clock (blue). The red dashed line equals  $3 \times 10^{-11}/\tau^{1/2}$ .

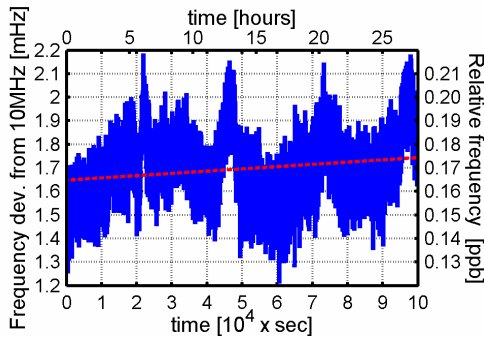


Figure 7. Frequency measurement of the 10 MHz output.

### IV. SUMMARY AND CONCLUSIONS

We have presented a  $^{87}\text{Rb}$  CPT based atomic clock which employs a small spherical glass vapor cell and a locking scheme based on FM spectroscopy. We described an empirical optimization of the FM parameters and the Lock-in amplifier reference phase that yield the largest slope in the spectrum of the Lock-in amplifier output. Since the accompanying noise was found to be independent of the FM parameters, the optimization yields the largest SNR. Scanning the 3.4173 GHz drive signal to the laser yields a resonance width of less than 190 Hz. One set of optimized FM parameters: modulation frequency of 870 Hz and an index of 0.5 were chosen for operation of the clock. The clock exhibits a short-term stability of  $3 \times 10^{-11}/\sqrt{\tau}$  for time constants of 0.5 sec to 200 sec and a long term frequency stability better than  $10^{-10}$  with a slow relative drift of  $10^{-11}/\text{day}$ . The clock performance is limited by the VCSEL noise and by environmental disturbances of the large laboratory set-up which mainly affect the long-term stability.

This work was performance within the framework of developing a miniature atomic clock. The authors thank Dr. A. Stern and Mr. B. Levi of AccuBeat Ltd. and prof. M. Rosenbluh of Bar-Ilan University.

### REFERENCES

- [1] J. Vanier, "Atomic clocks based on coherent population trapping: a review", *Appl. Phys. B.*, vol. 81, pp. 421-442, 2005.
- [2] S. Knappe, P.D.D. Schwindt, V. Shah, L. Liew, J. Moreland, L. Hollberg, and J. Kitching, "A chip-scale atomic clock based on  $^{87}\text{Rb}$  with improved frequency stability", *Optics express*, vol. 13, no. 4, pp. 1249-1253, February 2005.
- [3] R. Lutwak and P. Vlitaz and M. Varghese, M. Mescher and D. K. Serkland and G. M. Peake, "The MAC - a Miniature Atomic Clock" in *Proceedings of 2005 Joint IEEE International Frequency Control (UFFC) Symposium and the 37th Annual Precise Time & Time Interval (PTTI) Systems & Applications Meeting*, August 29-31, 2005, Vancouver, BC, Canada, pp. 752-757.
- [4] N. Cyr, M. Têtu and M. Breton, "All-optical microwave frequency standard: a proposal", *IEEE Trans. Instrum. Meas.*, vol. 42, no. 2, pp. 640-649, April 1993.
- [5] D. V. Kuskenskov, H. Temkin and S. Swirhun, "Polarization instability and relative intensity noise in vertical-cavity surface-emitting lasers", *Appl. Phys. Lett.*, vol. 67, pp. 2141-2143, October 1995.
- [6] V. Gerginov, V. Shah, S. Knappe, P. D. D. Schwindt, L. Hollberg and J. Kitching, "Atom-based stabilization for laser-pumped atomic clocks" in *Proceedings of the 20th European Frequency and Time Forum (EFTF)*, March 27-30, 2006, Braunschweig, Germany, pp. 224-228.
- [7] I. Ben-Aroya, M. Kahanov and G. Eisenstein, "A CPT based  $^{87}\text{Rb}$  atomic clock employing a small spherical glass vapor cell", in *Proceedings of the 38th Annual Precise Time & Time Interval (PTTI) Systems & Applications Meeting*, December 5-7, 2006, Reston, VA, USA, in press.
- [8] G. C. Bjorklund, M. D. Levenson, W. Lenth and C. Ortiz, "Frequency modulation (FM) spectroscopy - Theory of lineshapes and signal-to-noise analysis", *Appl. Phys. B.*, vol. 32, pp. 145-152, 1983.
- [9] M. Gehrtz, G. C. Bjorklund and E. A. Whittaker, "Quantum-limited frequency-modulation spectroscopy", *J. Opt. Soc. Am. B.*, vol. 2, no. 2, pp. 1510-1526, September 1985.
- [10] R. Wynands and A. Nagel, "Inversion of frequency-modulation spectroscopy line shapes", *J. Opt. Soc. Am. B.*, vol. 16, no. 10, pp. 1617-1622, October 1999.

- [11] J. Kitching, S. Knappe, N. Vukicevic, L. Hollberg, R. Wynands and W. Wiedmann, "A microwave frequency reference based on VCSEL-driven dark line resonances in Cs vapor", *IEEE Trans. Instrum. Meas.*, vol. 49, no. 6, pp. 1313-1317, December 2000.
- [12] J. Kitching, H. G. Robinson, L. Hollberg, S. Knappe and R. Wynands, "Optical-noise in laser-pumped, all-optical microwave frequency references", *J. Opt. Soc. Am. B.*, vol. 18, no. 11, pp. 1676-1683, November 2001.
- [13] I. Ben-Aroya, M. Kahanov and G. Eisenstein, "Characterization of FM spectroscopy parameters in a CPT based atomic clock: detailed analysis and experimental confirmation," unpublished.